PERGAMON

Chemical Engineering Science 58 (2003) 557–568

Chemical Engineering Science

www.elsevier.com/locate/ces

Molecular simulations in zeolitic process design

B. Smit, R. Krishna*

Department of Chemical Engineering, University of Amsterdam, Nieuwe Achtergracht 166, 1018 WV Amsterdam, The Netherlands

Abstract

Recent developments in molecular simulation techniques provide estimates of data, and valuable new insights, in the design of processes using zeolite adsorbents or catalysts. We illustrate these advances by considering a variety of examples such as separation of mixtures of linear and branched alkanes.

Configurational-bias Monte Carlo (CBMC) simulations allow accurate determination of the sorption isotherms of alkanes and their mixtures in various zeolites. The CBMC simulations reveal subtle entropy effects that allow separations of alkane mixtures on the basis of the degree of branching. Novel and efficient separation processes can be developed by exploiting such entropy effects.

Transition rate theories and molecular dynamics (MD) simulations allow the calculation of hopping rates of molecules and diffusivities within zeolites. Mixture diffusion in zeolites can be probed using kinetic Monte Carlo or MD simulations. These simulations help us understand the influence of correlations in molecular jumps. Such correlation effects have a profound influence on mixture diffusion characteristics.

For the design of zeolite-based processes, a multi-scale modelling strategy is suggested.

Keywords: Zeolites; Adsorption; Monte Carlo simulations; Molecular dynamics; Transition state theory; Alkane mixtures; Maxwell–Stefan theory; Diffusion

1. Introduction

Zeolites are crystalline nanoporous materials that are widely used in the chemical industry as catalysts and adsorbents (Kärger & Ruthven, 1992). Zeolite crystals are incorporated into binders and used in the form of pellets in fixed or simulated moving bed reactors. Alternatively, zeolite crystals are coated on to a porous membrane support and used in (catalytic) membrane reactors and separation devices. A wide variety of zeolite channel structures are encountered; for example, AFI consists of straight cylindrical channels, MFI consist of straight and zig-zag channels that intersect each other, FAU and LTA consist of cages that connect to one another through windows. For any given separation or reaction duty, there is an optimum zeolite structure offering the right product selectivity. Transport and chemical reactions of molecules within zeolites are significantly influenced by their sorption characteristics. Although experimental data are available on adsorption of pure components in various zeolites, experimental data on mixture sorption are very scarce; this scarcity of experimental data is due to the difficulty of experimentation with mixtures (Talu, 1998). In order to interpret the experimentally observed product distributions from zeolite catalysed processes, we need insights into the energetics and siting of intermediate molecular species formed during the reaction; such information is impossible to obtain from experiments.

Molecular simulations have played an important role in the past few years in developing our understanding of the relation between microscopic and macroscopic properties of guest molecules in zeolitic hosts (Fuchs & Cheetham, 2001). Molecular dynamics (MD), Monte Carlo (MC), transition state and rare event simulation techniques have been used to study sorption and diffusion in zeolites (Auerbach, 2000; Demontis & Suffritti, 1997; Frenkel & Smit, 2002; Keil, Krishna, & Coppens, 2000). It is the objective of this paper to highlight these advances and to show that molecular simulations can provide new insights not available from experiments and that they can provide clues to the development of novel separation and reaction processes.

* Corresponding author. Tel.: +31-20-525-7007; fax: +31-20-525-5604.
E-mail address: krishna@science.uva.nl (R. Krishna).

0009-2509/03/$ - see front matter © 2003 Elsevier Science Ltd. All rights reserved.
doi:10.1016/S0009-2509(02)00580-8

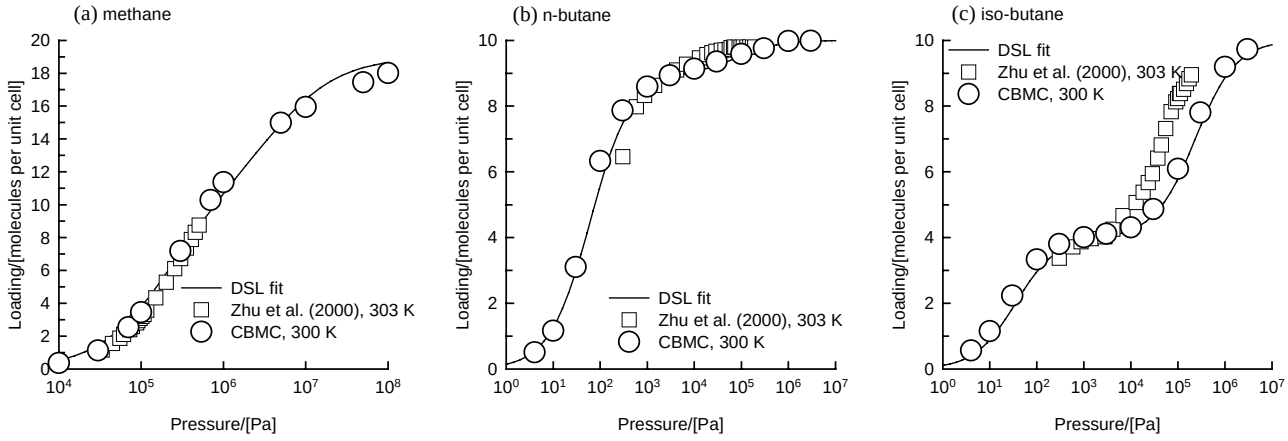

Fig. 1. Comparison of the experimental data for pure component isotherms for (a) methane, (b) *n*-butane and (c) *iso*-butane in MFI with CBMC simulations.

2. Simulation of adsorption in zeolites

2.1. Configurational-bias Monte Carlo (CBMC) simulation technique

In MC simulations the zeolite crystals are allowed to exchange molecules with a reservoir of molecules at a fixed chemical potential in the Grand-Canonical (or μ, V, T) ensemble. In this ensemble the temperature, volume, and chemical potential are fixed. The equilibrium conditions dictate that the temperature and chemical potential of fluid phase inside the zeolite and in the external reservoir must be equal. We therefore need to know only the μ and T of the gas in the reservoir in order to determine the equilibrium concentration of molecules within the zeolite; this equilibrium is not affected by say the resistance of the gas–zeolite interface to transport of molecules. In a MC simulation one does not have to follow the "natural" path of the molecule, as in a MD simulation, and one can perform "moves" to locate a molecule within an arbitrary position within the zeolite. This technique works very well for small molecules such as methane. For example, in an MC simulation for methane sorption, we observe that out of 1000 attempts to place a methane molecule to a random position within a zeolite, 999 attempts will be rejected because the methane molecule overlaps with an atom within the zeolite matrix. For ethane we have to insert two C atoms and, approximately, only 1 move in 10^6 attempts will be successful. Clearly, the strategy of randomly inserting molecules within a zeolite matrix will not work for long chain alkanes. To make MC simulations of long chain molecules feasible, the CBMC technique has been developed (Frenkel & Smit, 2002). The principle idea of the CBMC technique is to grow an alkane chain, atom by atom, instead of attempting to insert the entire molecule at random. This growing procedure introduces a bias that can be removed exactly by adjusting the acceptance rules. Computational details of the implementation of the CBMC algorithm are to be found in Vlugt, Martin, Smit, Siepmann, and Krishna (1998).

A simple approach to describe the alkane molecules is to use the *united-atom model*, in which CH_3, CH_2, and CH groups are considered as single pseudo-atoms with interactions described by a Lennard–Jones potential. The bonded interactions include bond-bending and torsion potentials; details for the alkane model can be found in Vlugt, Krishna, and Smit (1999). Most simulation studies follow the approach of Kiselev and assume the zeolite lattice to be *rigid* and that interactions of an alkane with the zeolite are dominated by the dispersive forces between pseudo-atoms of the alkane and the oxygen atoms of the zeolite. The total interaction energy is represented by two terms: an attractive term and a repulsive term, and are described by a Lennard–Jones potential; the potential parameters are usually obtained by fitting to experimental heats of adsorption and Henry coefficients (Vlugt et al., 1999).

2.2. Sorption isotherms for pure alkanes

Let us first validate the accuracy of CBMC simulations by comparison with experiments. CBMC simulations for sorption of methane (C1), *n*-butane (*n*C4) and *iso*-butane (*i*C4) in MFI zeolite (silicalite-1) at 300 K are shown in Fig. 1; these simulations are in very good agreement with experimental data (Zhu, Kapteijn, & Moulijn, 2000). The agreement between CBMC simulations and experiments observed in Fig. 1 is typical for linear and branched alkanes in the 1–10°C atoms range in MFI (Vlugt et al., 1999; Schenk, Vidal, Vlugt, Smit, & Krishna, 2001). An important advantage of CBMC simulations is that they provide much more insight into sorption behaviour than available from experiments alone. For example, the sorption isotherm for *i*C4 shows a pronounced inflection at a loading $\Theta = 4$ molecules per unit cell (see Fig. 1(c)). Up to a system

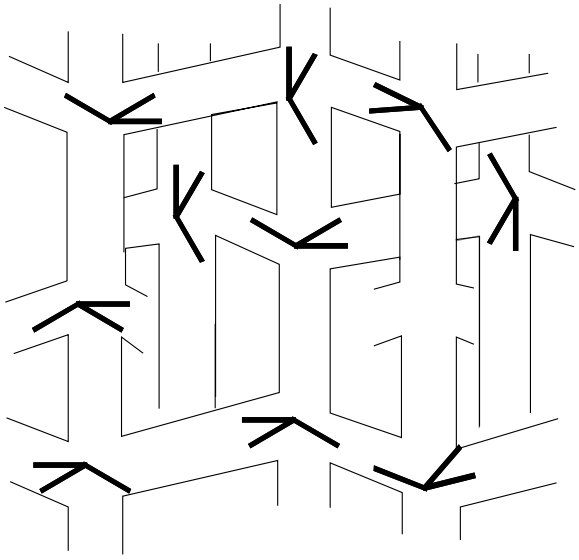

Fig. 2. Schematic showing preferential location of *iso*-butane molecules at the intersections between the straight and zig-zag channels of MFI.

pressure of 1 kPa, the isobutene molecules are exclusively located at the intersections, that have a maximum capacity of 4 molecules/unit cell; see Fig. 2 for a snapshot of the siting of *i*C4 molecules. Loadings in excess of 4 molecules/unit cell can only be achieved by pushing *i*C4 into the straight and zig-zag channels. Only when the pressure is significantly increased beyond 10 kPa, the zig-zag channels and straight channels tend to get occupied. Due to its branched configuration, isobutane demands an extra "push" to locate within the channel interiors. This extra push is the root cause of the inflection behaviour.

Interestingly, *n*-hexane also shows a slight inflection at a loading of 4 molecules/unit; this inflection is due to "commensurate" freezing caused by the fact that the length of the *n*-hexane molecule is commensurate with the length of the zig-zag channel. All mono-branched alkanes, in the 5 –8°C atoms range are found to exhibit inflection behaviour (Schenk et al., 2001; Vlugt et al., 1999); witness for example the inflection behaviour exhibited by 2-methylpentane (2MP) and 3-methylpentane (3MP) in MFI zeolite (see Fig. 3(a)). Just as in the case of isobutane, 2MP prefers the locate at the intersections due to the availability of extra "leg room"; the 2MP molecule has its branched end at the intersections and sticks its leg out in either the straight or zig-zag channels. Di-branched alkanes, typified by 2,2dimethyl butane (22DMB) and 2,3dimethyl butane (23DMB), also prefer to locate at the intersections of MFI. However, these molecules are much bulkier than mono-branched alkanes and, consequently, they cannot be pushed into the channel interiors. The maximum loading of di-branched alkanes, such as 22DMB, in MFI is restricted to 4 molecules/unit cell (see Fig. 3(b)). The inflection behaviour of mono-branched alkanes in MFI at a loading of 4 molecules/unit cell, as well as the restriction of the maximum loading of di-branched alkanes to this loading, is a consequence of configurational differences. This *configurational entropy* effect causes the saturation loadings of hexane isomers in MFI to follow the hierarchy linear > mono-branched > di-branched.

From an engineering point of view it is important to obtain a good analytic description of the pure component isotherms for linear and branched alkanes; this is provided by dual-site Langmuir (DSL) model. In this model, the loading, $\Theta_i^0(P)$, expressed in molecules per unit cell is expressed as a

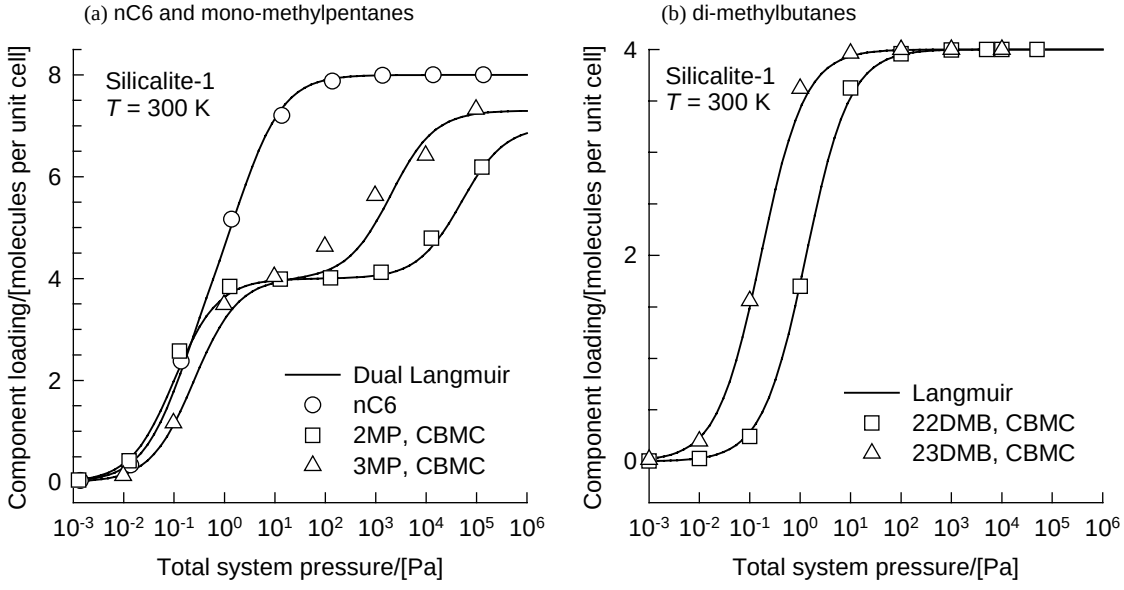

Fig. 3. CBMC simulations of pure component isotherm for (a) *n*C6, 2MP, 3MP and (b) 22DMB and 23DMB in MFI at 300 K.

Table 1
Pure component parameters for DSL model

Component i	Temperature (K)	Dual-site Langmuir parameters (see Eq. (1)) Site A		Site B	
		$b_{i,A}$ (Pa^{-1})	$\Theta_{i,\mathrm{sat},A}$ (molecules/unit cell)	$b_{i,B}$ (Pa^{-1})	$\Theta_{i,\mathrm{sat},B}$ (molecules/unit cell)
C1	300	4.87×10^{-6}	11.0	2.38×10^{-7}	8.0
C2	300	9.73×10^{-5}	12.0	4.38×10^{-7}	3.0
C3	300	9.64×10^{-4}	11.0	5.06×10^{-6}	1.0
*n*C4	300	1.626×10^{-2}	9.0	1.14×10^{-5}	1.0
*i*C4	300	2.84×10^{-2}	4.0	4.28×10^{-6}	6.0
*n*C6	300	7.0	4.0	0.4	4.0
2MP	300	10.0	4.0	2.0×10^{-5}	3.0
*n*C6	362	6.32×10^{-2}	4.0	1.7×10^{-3}	4.0
3MP	362	4.75×10^{-2}	4.0	2.27×10^{-5}	2.3
22DMB	362	1.085×10^{-2}	4.0	—	—

function of pressure P as follows:

$$\Theta_i^0(P) = \frac{\Theta_{i,\mathrm{sat},A} b_{i,A} P}{1 + b_{i,A} P} + \frac{\Theta_{i,\mathrm{sat},B} b_{i,B} P}{1 + b_{i,B} P}. \quad (1)$$

The superscript 0 on $\Theta_i^0(P)$ is used to emphasize that the relation is for *pure* component loadings. In Eq. (1) $b_{1,A}$ and $b_{1,B}$ represent the DSL model parameters expressed in Pa^{-1} and the subscripts A and B refer to two sorption sites within the MFI structure, with different sorption capacities and sorption strengths. The $\Theta_{i,\mathrm{sat},A}$ and $\Theta_{i,\mathrm{sat},B}$ represent the saturation capacities of sites A and B, respectively. It is to be noted that the total saturation loading $\Theta_{i,\mathrm{sat}} = \Theta_{i,\mathrm{sat},A} + \Theta_{i,\mathrm{sat},B}$ is not a fitted parameter but taken from the final plateau value of the sorption isotherm, estimated from CBMC simulations. The fitted isotherms are seen to fit the isotherms very well (see Figs. 1 and 3) (the DSL parameters are specified in Table 1).

Having established that we can reproduce the experimental adsorption isotherms in MFI, we can study the sorption behaviour in zeolites that have received much less experimental attention. For MFI we demonstrated the importance of *configurational entropy* effects; for other zeolitic structures these effects may act in a completely different manner. For example, consider the sorption of hexane isomers, *n*C6, 3MP, 22DMB and 23DMB in AFI; the CBMC simulations of the component loadings at 403 K are shown in Fig. 4. The sorption hierarchy is found to be di-branched > mono-branched > linear which is opposite to the hierarchy for MFI. AFI consists of cylindrical channels of 0.73 nm radius. The channel dimension is large enough to accommodate the bulky 22DMB and 23DMB and there is therefore no configurational penalty for these molecules. However, the length of the molecules decreases with increased degree of branching (see Fig. 5); this implies that number of molecules that can be accommodated into the channels increases with the degree of branching. The increased sorption strength with increased branching can be termed a *length entropy* effect, arising as it does as a consequence of decreasing linear dimension of the molecule.

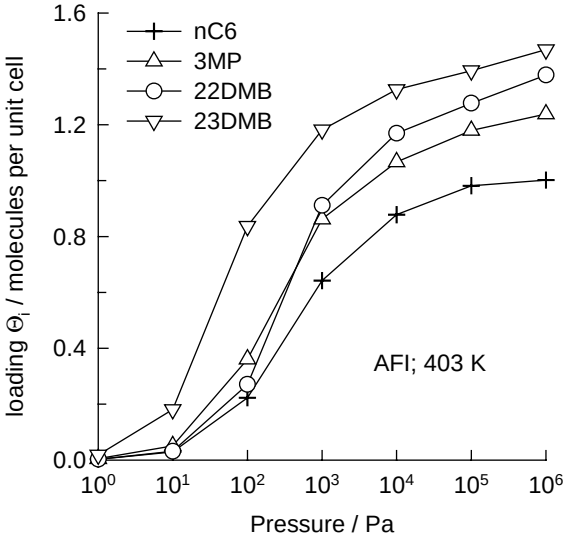

Fig. 4. Sorption isotherms for *n*C6, 3MP, 22DMB and 23DMB in AFI at 403 K determined by CBMC simulations.

2.3. Size entropy effects during mixture sorption

Most practical applications of zeolites involve mixtures, for which there is little experimental data. Consequently, engineers have resorted to estimations of sorption selectivities in mixtures for purposes of screening zeolites. For example, the sorption selectivity of *mixtures* is often estimated on the basis of the values of the Henry coefficients, i.e. the sorption strengths of the pure components at near-zero loadings (Denayer, Baron, Martens, & Jacobs, 1998; Huddersman & Klimczyk, 1996). We shall demonstrate below that using Henry coefficients to estimate the sorption selectivity of

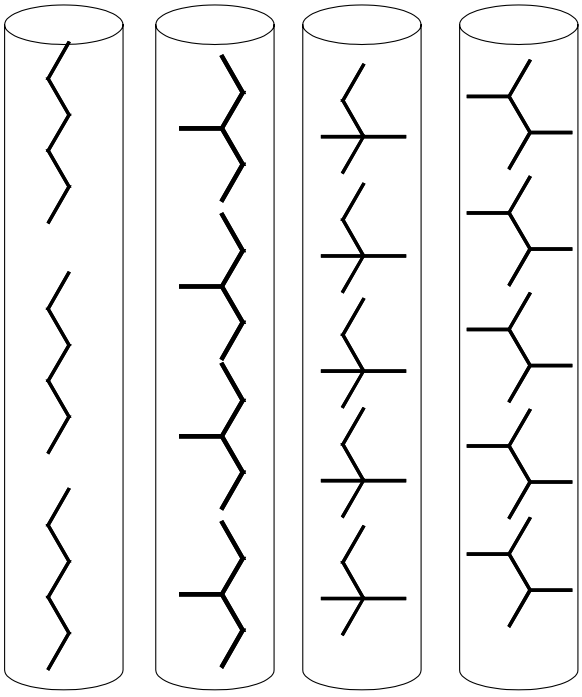

Fig. 5. Schematic of length entropy effect during adsorption of *n*C6, 3MP, 22DMB and 23DMB in the cylindrical channels of AFI.

mixtures can lead to completely wrong conclusions regarding separation possibilities. Let us first consider sorption of a 95–5 mixture of methane (C1) and *n*-butane (*n*C4) in MFI at 300 K. The component loadings in the mixture Θ_i have been determined by Krishna, Calero, and Smit (2002) and are shown in Fig. 6(a). The sorption selectivity, defined by $S = \Theta_1/\Theta_2/p_1/p_2$ where Θ_i and p_i represent, respectively, the component loading and partial pressure in the gas phase, is shown in Fig. 6(b) as a function of the mixture loading ($\Theta_{\text{mix}} = \Theta_1 + \Theta_2$). It is interesting to note that the sorption selectivity for *n*C4 with respect to C1 decreases significantly from the value dictated by the Henry coefficients (indicated by dashed line) when the mixture loading Θ_{mix} is increased beyond 8 molecules/unit cell. The reason for this selectivity decrease lies in the fact that near saturation loadings the vacant sites within MFI are more easily filled up with the smaller C1 molecule than with the bulkier *n*C4 molecules. This is a *size entropy* effect. Both component loadings and the sorption selectivity are very well predicted by the ideal adsorbed solution theory (IAST), developed by Myers and Prausnitz (1965) (see Fig. 6).

MFI membrane permeation data for C1/C2, C1/C3, C2/C4, and *C*1/*n*C4 mixtures in published literature (Kapteijn, Moulijn, & Krishna, 2000; Krishna, 2001; van de Graaf, Kapteijn, & Moulijn, 1999) provide confirmation, albeit indirect, of the importance of size entropy effects at high loadings.

2.4. Configurational entropy effects in mixture sorption

Let us now consider the separation of hexane isomers, *n*C6 and 2MP, an important separation problem in the petroleum industry. The Henry coefficients of these components at 300 K in MFI are estimated from molecular simulation techniques to be 3.38 and 4.47 mol/kg/Pa, respectively. The sorption selectivity S for a 50–50 mixture is therefore equal to 0.76, which is too low to be exploited in practice. CBMC simulations for component loadings of a 50–50 mixture of *n*C6 and 2MP in MFI at a temperature of 300 K are shown in Fig. 7(a) for a wide range of total system pressures P. It is interesting to note the maximum in the loading of 2MP at about 5 Pa. When the pressure is raised above 50 Pa the

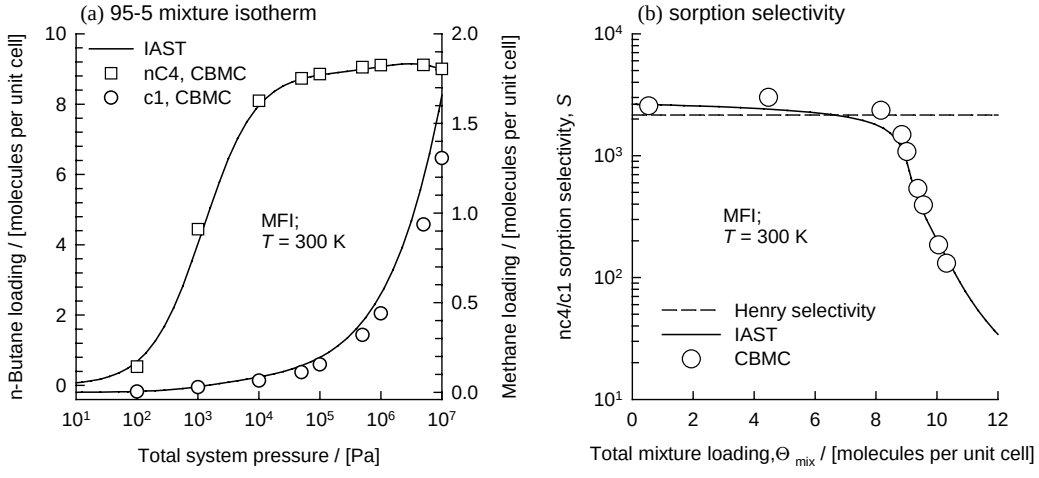

Fig. 6. (a) Sorption loadings of 95–5 mixture of C1 and *n*C4 in MFI at 300 K and (b) *n*C4/C1 sorption selectivity. The sorption selectivity based on Henry coefficients is indicated by the dashed line.

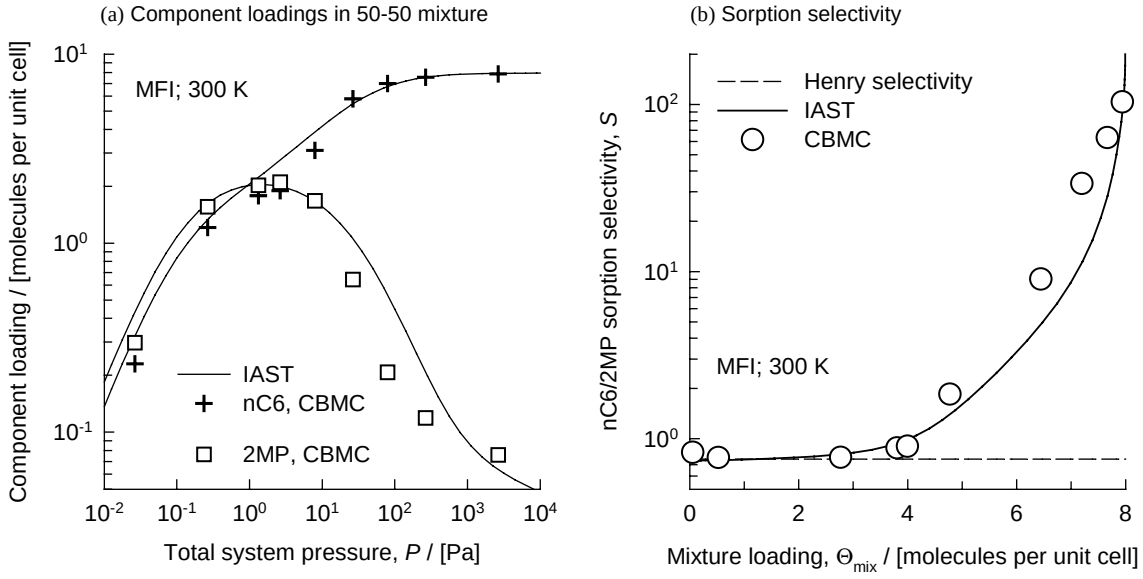

Fig. 7. (a) CBMC simulations of 50–50 mixture isotherm for *n*C6–2MP in MFI at 300 K. (b) Sorption selectivity as a function of total system pressure. The sorption selectivity based on Henry coefficients is indicated by the dashed line.

loading of 2MP reduces virtually to zero. The *n*C6 molecules fit nicely into both straight and zig-zag channels, whereas the 2MP molecules are preferentially located at the intersections between the straight channels and the zig-zag channels. Below a total loading of 4 molecules/unit cell, there is no real competition between *n*C6 and 2MP. The *n*C6 locates within the channels and 2MP at the intersections. When all the intersection sites are occupied, to further adsorb 2MP, we need to provide an extra "push". Energetically, it is more efficient to obtain higher mixture loadings by "replacing" the 2MP with *n*C6; this *configurational entropy* effect is the reason behind the curious maxima in the 2MP loading in the mixture. The *n*C6/2MP sorption selectivity is plotted in Fig. 7(b). We see that the sorption selectivity increases from near-unity values for $\Theta_{\mathrm{mix}} < 4$ to values of around 100 near saturation loadings. Clearly, the Henry selectivity values (denoted by the dashed lines in Fig. 7(b)) are too pessimistic and ignore a potentially attractive separation possibility at high mixture loadings. We also note in Fig. 7 that the IAST does a good job of predicting both the component loadings and the sorption selectivity for this mixture; the predictions are based on the DSL parameters specified in Table 1.

The CBMC simulation technique can be easily extended to multi-component mixtures and allows us to mimic a more realistic separation task. For example, the sorption hierarchy in MFI for a five-component equimolar mixture of hexane isomers consisting of *n*C6, 2MP, 3MP, 22DMB and 23DMB, at high mixture loadings, is *n*C6 $\gg$ 2MP $\approx$ 3MP $\gg$ 22DMB $\approx$ 3DMB; see CBMC simulation results in Fig. 8(a). Hexane isomers can therefore be separated into three fractions consisting of linear, mono-branched and di-branched alkanes; experimental evidence in the literature to confirm this separation possibility is available (Calero, Smit, & Krishna, 2001a, b; Santilli, 1986). An important objective in catalytic isomerization process is to achieve such a separation hierarchy starting with a mixture say in the 5–7 C atoms range. The di-branched alkanes are the desired products and the linear and mono-branched alkanes need to be recycled to the isomerization reactor. CBMC simulations for mixture of linear, mono-branched and di-branched alkanes in the 5–7 C atom range in MFI at 300 K are shown in Fig. 8(b). At low loadings (i.e. low pressures) we see that the sorption hierarchy is dictated by the number of C atoms, i.e. C7 isomers $\gg$ C6 isomers $\gg$ C5 isomers. Operating at low loadings does not yield the desired separation depending on the degree of branching. However, for mixture loadings approaching 8 molecules/unit cell, the situation changes dramatically; see the right end of Fig. 8(b). We see that the separation hierarchy is now linear $\gg$ mono-branched $\gg$ di-branched, exactly as desired.

3. Molecular simulations of diffusivities in zeolites

Diffusion in zeolites can be studied using MD simulations, transition state theories (TST) or kinetic Monte Carlo (KMC) simulations (Keil et al., 2000). MD simulation techniques are viable only for relatively small molecules such as methane, or at conditions for which long chain alkanes diffuse sufficiently rapidly (Webb, Grest, & Mondello, 1999). For many systems the molecules diffuse very slowly in the pores of a zeolite and as a consequence the total simulation time needed to compute a diffusion coefficient can become prohibitively large. Often such low diffusion coefficients are the consequence of "diffusion barriers" such as narrow

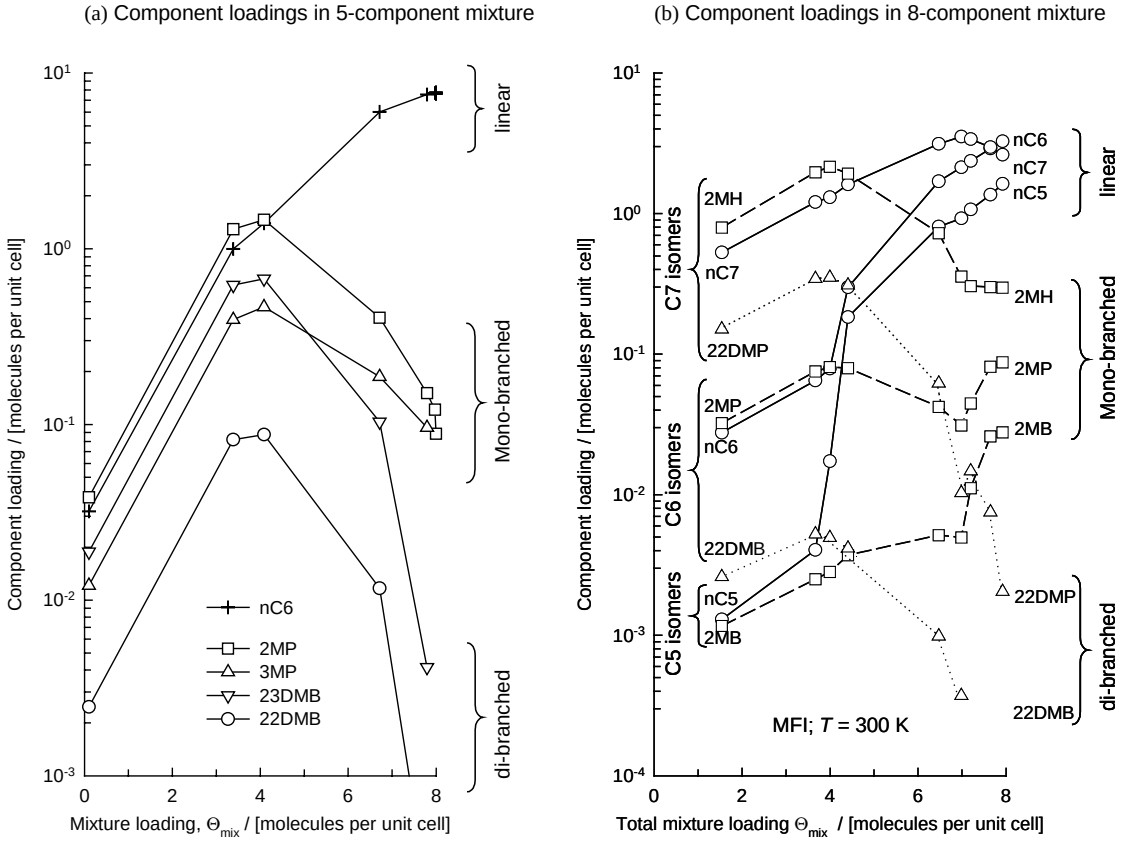

Fig. 8. (a) CBMC simulations of component loadings for equimolar five-component mixture of nC$_6$, 2MP, 3MP, 22DMB and 23DMB in MFI at 300 K as a function of total mixture loading Θ_{mix}. (b) Component loadings in an equimolar eight-component mixture nC5–2MB–nC6–2MP–22DMB–nC7–2MH–22DMP at 300 K in MFI as a function of total mixture loading Θ_{mix}.

windows between cages. For those systems diffusion can be seen as a hopping process, if the molecule has sufficiently high kinetic energy it may jump from one cage to another. These hopping rates can be computed using rare event simulation techniques (Frenkel & Smit, 2002), in which the free energy of the diffusion barrier is computed together with the transmission coefficient. These techniques have been use to compute the diffusion coefficient of bulky rigid molecules, such as benzene (see Auerbach (2000) for a review), but can also be applied to flexible chain molecules.

In practice, we require to estimate the "transport" or Fick diffusivities at finite loadings. For example, the Fick diffusivity D_1 for CH$_4$ in silicalite-1 increases strongly with molecular loading; see Fig. 9(a) for the simulation results of Maginn (1993) and Skoulidas and Sholl (2001). Using the Maxwell–Stefan (M–S) theory, that is based on the theory of irreversible thermodynamics, the Fick diffusivity D_1 can be related to the M–S diffusivity Đ$_1$ by

$$D_1 = Đ_1 \Gamma, \qquad \Gamma = \frac{\partial \ln p_1}{\partial \ln \Theta_1}, \tag{2}$$

where Γ, the thermodynamic correction factor, can be determined from the sorption isotherm; for a Langmuir isotherm, $\Gamma = 1/(1-\Theta_1/\Theta_{1,\mathrm{sat}})$. For weakly confined molecules such as CH$_4$ in silicalite-1 the M–S Đ$_1$ is independent of loading (see Fig. 9(b)) and the Fick D_1 follows the behaviour predicted by Eq. (2). For strongly confined molecules, the M–S Đ$_1$ often exhibits a linear decline with loading Θ_1 following $Đ_1 = Đ_1(0)(1-\Theta_1/\Theta_{1,\mathrm{sat}})$ and in this case the Fick D_1 is practically independent of loading. Mixture diffusion in zeolites is a strongly coupled process; the coupling arises due to correlations in the molecular jumps. Due to correlation effects, the species with the higher mobility is slowed down; conversely the species with the lower mobility is speeded up. Correlation effects are accounted by introducing "exchange" coefficients Đ$_{ij}$ in the M–S formulation

$$-\rho\frac{\theta_i}{RT}\nabla\mu_i = \sum_{\substack{j=1\\ j\neq 1}}^{n}\frac{\Theta_j \mathbf{N}_i - \Theta_i \mathbf{N}_j}{\Theta_{i,\mathrm{sat}}\Theta_{j,\mathrm{sat}}Đ_{ij}} + \frac{\mathbf{N}_i}{\Theta_{i,\mathrm{sat}}Đ_i},$$

$$i = 1,2,\ldots,n. \tag{3}$$

The interchange coefficient Đ$_{ij}$ can be estimated by the logarithmic interpolation formula (Krishna & Wesselingh, 1997)

$$Đ_{ij} = [Đ_i]^{\theta_i/(\theta_i+\theta_j)}[Đ_j]^{\theta_j/(\theta_i+\theta_j)}. \tag{4}$$

Correlation effects during mixture diffusion can be studied conveniently using either MD or KMC simulations.

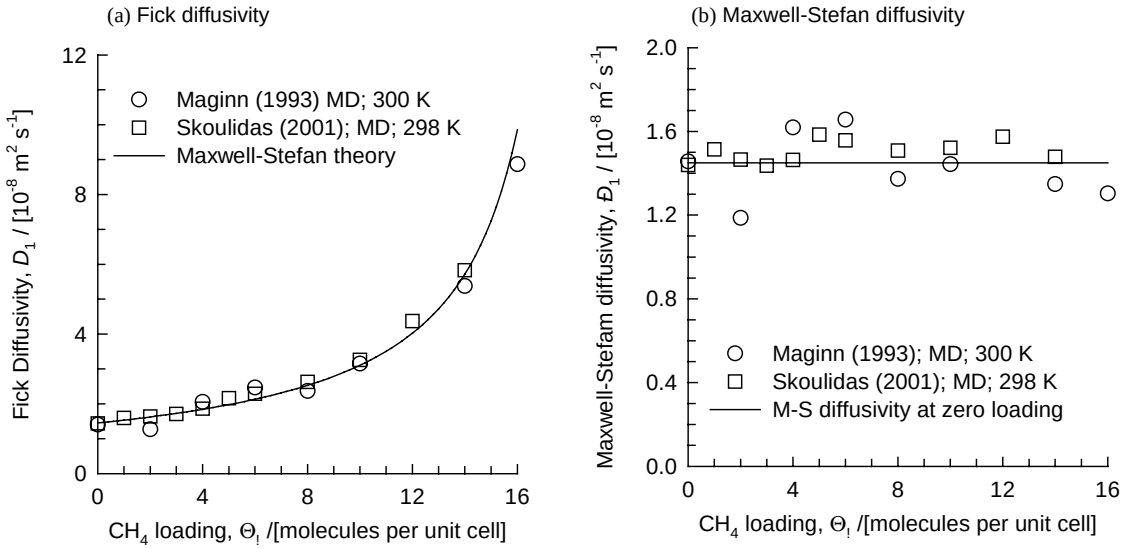

Fig. 9. (a) Fick diffusivity for CH_4 in silicalite-1 at 298 and 300 K as a function of molecular loading. MD simulation data of Skoulidas and Sholl (2001) and Maginn, Bell, and Theodorou (1993). (b) M–S diffusivity for CH_4 a function of molecular loading.

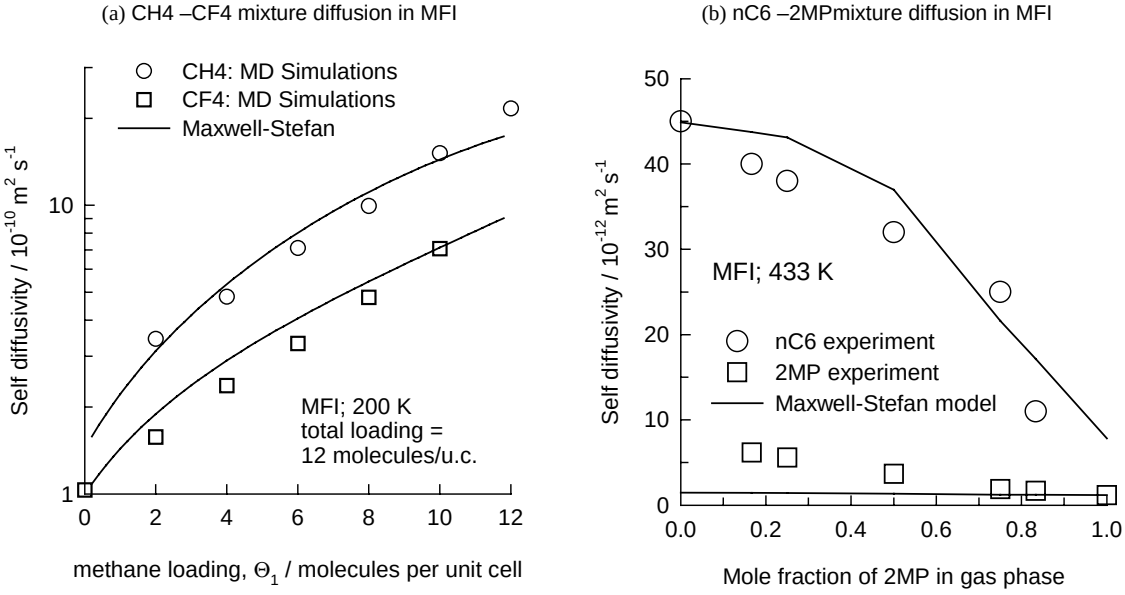

Fig. 10. (a) Comparison of MD binary mixture simulations of Snurr and Kärger (1997) for self diffusivities of CH_4 and CF_4 in MFI at 200 K with the predictions of the M–S theory. (b) Experimental data of Schuring, Koriabkina, de Jong, Smit, and van Santen (2001) for self-diffusivities in MFI of the mixture of *n*-hexane (*n*C6, component 1) and 2-methylpentane (2MP, component 2) are compared with the predictions of the M–S theory.

The validity of Eq. (4) has also been established by means of MD and KMC mixture simulations (Krishna, 2002; Krishna & Paschek, 2002). Consider the MD simulations for self-diffusivities in a mixture of CH_4 (component 1) and CF_4 (component 2) in MFI zeolite at 200 K (Snurr & Kärger, 1997). The MD simulations were carried out at a total mixture loading of $\Theta_1 + \Theta_2 = 12$ molecules/unit cell and the methane loading is varied from 0–12 molecules/unit cell; their simulation data are shown as open symbols in Fig. 10(a). The CH_4 diffusivity decreases sharply with increasing concentration of CF_4 in the mixture. Conversely, the CF_4 diffusivity increases significantly with increasing concentration of CH_4 in the mixture. The M–S theory is able to predict mixture diffusion behaviour with good accuracy. Published experimental data of Schuring, Koriabkina, de Jong, Smit, and van Santen (2001) for self-diffusion in a mixture of *n*C6–2MP confirm the strong retarding influence of 2MP on the mobility of *n*C6; this retardation effect is very well modelled by the M–S model; (see Fig. 10(b)).

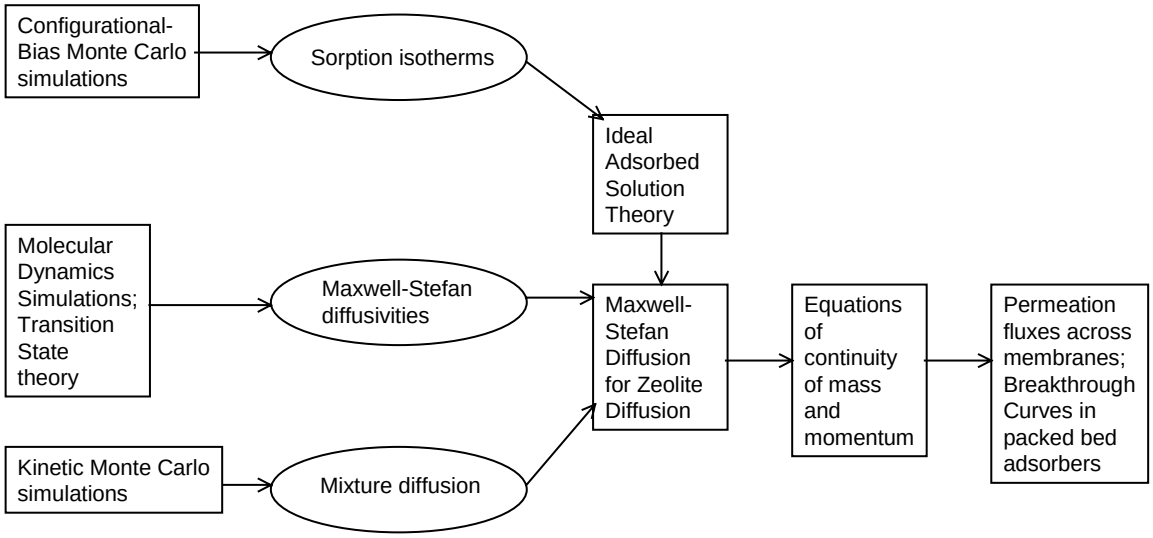

Fig. 11. Multi-scale modelling strategy for zeolitic process design.

4. Process design

For design of a zeolite-based separation process, the multi-scale strategy outlined in Fig. 11 can be followed. This strategy consists of the following steps:

(1) Calculating the sorption isotherms of the pure components and the mixtures using CBMC techniques. The pure component isotherms are fitted using say the DSL isotherm. Mixture isotherms are estimated using the IAST, and verified using CBMC.
(2) Determination of the M–S diffusivities from MD or TST,
(3) Using KMC simulation techniques for studying and verifying the mixture diffusion rules following the M–S theory. In particular, the estimation of the interchange coefficient $Đ_{ij}$ using Eq. (4) needs to be tested for the particular mixture in the specific zeolite topology.
(4) Solving the transient equations of continuity of mass for each species, along with the M–S equations describing intra-crystalline diffusion, to obtain the transient permeation fluxes in either packed bed adsorbers or across zeolite membrane devices.

In order to illustrate the strategy outlined in Fig. 11 we shall consider a few illustrative examples.

4.1. Permeation of methane and n-butane across MFI membrane

The permeation flux is obtained by solving the following set of two partial differential equations (PDE):

$$\frac{\partial \theta_i}{\partial t} = -\frac{1}{\rho \Theta_{i,\mathrm{sat}}} \frac{\partial N_i}{\partial z}, \tag{5}$$

where Eq. (3) describes the individual fluxes. For single-component permeation of C1 and *n*C4 with an upstream partial pressure of 50 kPa, maintaining the downstream partial pressures at vanishing values, the transient fluxes are shown in Fig. 12(a). We use the MS diffusivities for C1 to be $Đ_1 = 10^{-9}$ m^2/s and for *n*C4 we take $Đ_2 = 10^{-11}$ m^2/s following published experimental data (Bakker, 1999). The DSL isotherm parameters are as reported in Table 1. At steady state, the permeation flux of methane is 19.46 mmol/m^2/s and that of *n*C4 is 4.65 mmol/m^2/s because of its much lower diffusivity value. The permeation selectivity, S_P, defined by

$$S_P = \frac{N_2/N_1}{p_{20}/p_{10}} \tag{6}$$

is $4.65/19.46 = 0.239$. For binary mixture permeation, each component with 50 kPa upstream partial pressures, the transient fluxes are shown in Fig. 12(b). The mixture isotherm is predicted using IAST. The steady-state permeation selectivity is found to be 197, emphasizing that mixture permeation cannot be simply related to single-component permeation. Diffusion and sorption are closely interlinked. The more strongly adsorbed *n*C4 has a higher occupancy within the zeolite. The higher the occupancy, the higher the permeation rate. Futhermore, due to the interchange, expressed in Eq. (5), the more mobile C1 is slowed down by *n*C4. These two effects combine to yield a permeation selectivity of 197 in place of 0.239. In Fig. 12(c) the calculations of the permeation selectivity are compared with the experimental results obtained for a variety of upstream pressures by Bakker (1999); the agreement is good considering that virtually no empirical inputs were required in the model. The decrease in the selectivity with increasing butane partial pressure is a consequence of size entropy effects. Such size entropy

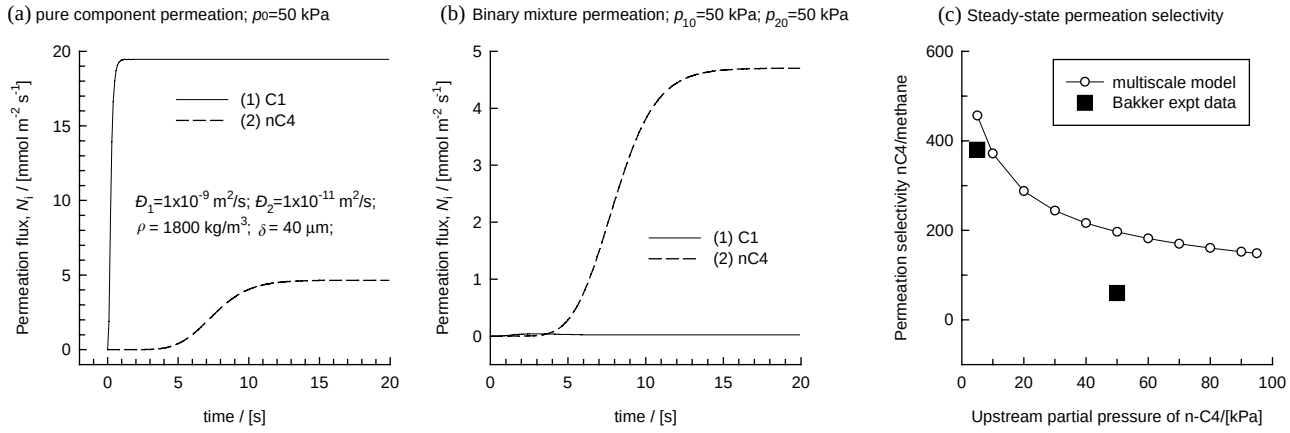

Fig. 12. (a) Transient permeation of pure components C1 and *n*C4 across MFI membrane at 300 K. The upstream partial pressure is maintained at 50 kPa. (b) Transient permeation across MFI membrane of 50–50 mixture of C1 and *n*C4 in MFI at 300 K. The partial pressures are maintained at 50 kPa in the upstream compartment. (c) Dependence of *n*C4/C1 permeation selectivity on the upstream partial pressure of *n*C4 when the total upstream pressure is maintained at 100 kPa. Also shown are the experimental data of Bakker (1999).

effects are properly accounted for by the IAST that has been used to describe the mixture thermodynamics.

4.2. Breakthrough of methane, ethane, propane and n-butane in packed adsorber

Assuming plug flow, the concentration at any position and instant of time is obtained by solving the following set of PDEs:

$$\frac{\partial c_i}{\partial t} = -\frac{\partial (u c_i)}{\partial z} - \left(\frac{1-\varepsilon}{\varepsilon}\right)\rho \frac{\partial \bar{q}_i}{\partial t}, \tag{7}$$

where c_i is the molar concentration in the gas phase, u is the fluid phase (absolute) velocity, z is the axial coordinate distance, ε is the bed porosity, ρ is the density of the zeolite crystals and $\bar{q}_i$ is the average molar loading, expressed in mol/kg, within the spherical particle given by

$$\bar{q}_i = \frac{3}{r_c^3}\int_0^{r_c} q_i r^2 \, \mathrm{d}r, \tag{8}$$

where r_c is the radius of the MFI crystallites embedded in the supporting matrix. Usually, the LDF approximation is made in order to avoid solving the intra-particle diffusion numerically. Furthermore, published models for breakthrough in packed beds (Ruthven, Farooq, & Knaebel, 1994) almost invariably use the multi-component Langmuir isotherm to describe mixture diffusion. Use of either LDF or the multi-component Langmuir isotherm is not to be recommended in the general case where subtle entropy effects come into play, affecting sorption and diffusion. For accurate modelling, therefore, there is no avoiding use of the IAST and using a rigorous solution of intra-crystalline diffusion using the M–S equations.

Consider the breakthrough behaviour for an equimolar mixture of methane (C1), ethane (C2), propane (C3) and *n*-butane (*n*C4) in an adsorber packed with MFI crystals operating at 300 K. The isotherm parameters are given in Table 1. As is conventional we plot in Fig. 13 the normalized concentrations of the two components at the exit, as a function of the dimensionless time tu_0/L where u_0 is the interstitial gas velocity at the inlet to the packed bed. It is clear that it is possible to separate pure methane from the quaternary mixture during the early stages of the breakthrough.

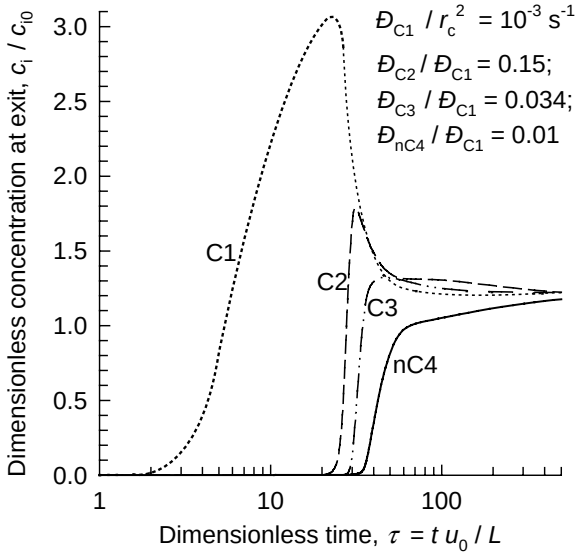

Fig. 13. Breakthrough of an equimolar mixture of C1, C2, C3 and *n*C4 at the exit of an adsorber packed with MFI crystals. The temperature $T = 300$ K; the porosity of the packed bed $\varepsilon = 0.4$; length of packed bed $L = 0.4$ m; interstial gas velocity at inlet $u_0 = 0.05$ m/s; density of MFI $\rho = 1800$ kg/m^3. The radius of the crystallites r_c was chosen such that $Đ_{C1}/r_c^2 = 10^{-3}$ s^{-1}. The initial loadings of the MFI crystals correspond to equilibrium at partial pressures of C1, C2, C3 and *n*C4 at 20 Pa. At time $t = 0$, the partial pressures of the adsorbing species at the inlet is maintained, $p_{i0} = 20$ kPa. The partial pressures of the non-adsorbing inerts are maintained such that the total pressure is 100 kPa.

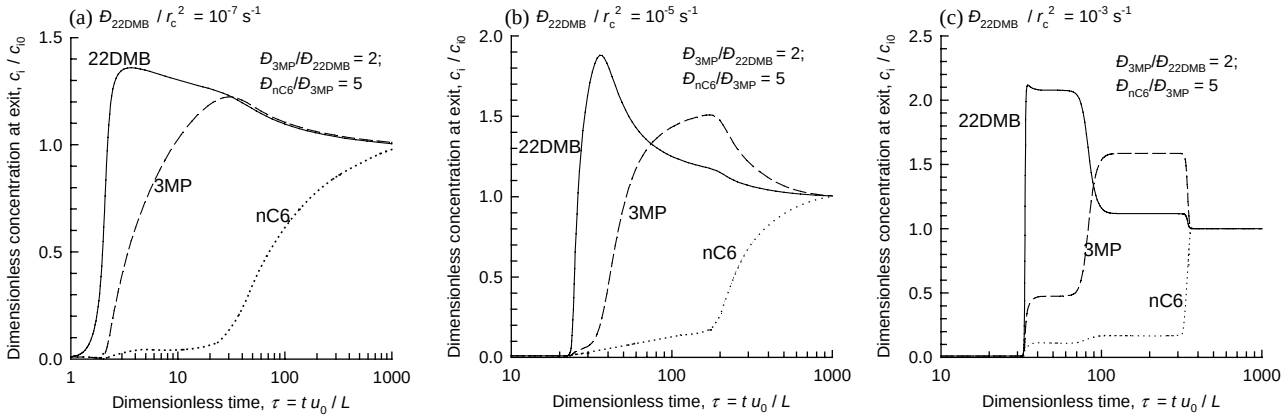

Fig. 14. Breakthrough of an equimolar mixture of *n*C6, 3MP and 22DMB at the exit of an adsorber packed with MFI crystals. The temperature $T = 362$ K; the porosity of the packed bed $\varepsilon = 0.4$; length of packed bed $L = 0.4$ m; interstial gas velocity at inlet $u_0 = 0.0125$ m/s; density of MFI $\rho = 1800$ kg/m^3. The radius of the crystallites r_c was chosen such that (a) $Đ_{C1}/r_c^2 = 10^{-7}$ s^{-1}, (b) $Đ_{C1}/r_c^2 = 10^{-5}$ s^{-1}, (c) $Đ_{C1}/r_c^2 = 10^{-3}$ s^{-1}. The initial loadings of the MFI crystals correspond to equilibrium at partial pressures of C1, C2, C3 and *n*C4 at 200 Pa. At time $t = 0$, the partial pressures of the adsorbing species at the inlet are maintained, $p_{i0} = 20$ kPa. The partial pressures of the non-adsorbing inerts are maintained such that the total pressure is 100 kPa.

4.3. Breakthrough of *n*C6, 3MP and 22DMB in packed adsorber

Consider the breakthrough behaviour for an equimolar mixture of *n*C6, 3MP and 22DMB in an adsorber packed with MFI crystals operating at 362 K. The isotherm parameters are given in Table 1. In order to ensure good separation, it is initial to preload the zeolites so that the mixture loading is maintained at a loading higher than 4 molecules/unit cell; the initial loading corresponds to equilibrium at partial pressures of 200 Pa of each of the isomers. Fig. 14 shows the breakthrough behaviours for three different crystallite sizes, described by (a) $Đ_{22DMB}/r_c^2 = 10^{-7}$ s^{-1}; (b) $Đ_{22DMB}/r_c^2 = 10^{-5}$ s^{-1}; (c) $Đ_{22DMB}/r_c^2 = 10^{-3}$ s^{-1}. Clearly, large crystallite sizes and operation under the diffusion controlled regime are desirable for separating 22DMB from the hexane isomeric mixture. If conditions are chosen such that $Đ_{22DMB}/r_c^2 = 10^{-7}$ s^{-1}, it is clear that during the initial transience of the breakthrough, it is possible to separate pure 22DMB from the mixture. This is the separation that is desirable in practice, because the linear and mono-branched isomers can then be recycled back to the catalytic isomerization reactor.

4.4. Breakthrough of *n*C6, 3MP and 22DMB in pulsed chromatograph

Another mode of separating hexane isomers is to employ a pulsed chromatographic operation. Fig. 15 shows the breakthrough in a chromatograph packed with MFI crystals operating at 362 K. Again the MFI are initially equilibrated with an equilibrium mixture with 200 Pa partial pressures each. A pulse consisting of a mixture of *n*C6, 3MP and 22DMB at partial pressures of 20 Pa, 20 kPa and 20 kPa, respectively, is injected through the chromatograph for a period of 50 s. After this 50 s, the chromatograph is swept with (nearly) pure *n*C6, that plays the role of desorbent. We note that 22DMB is virtually completely excluded from the mixture and breaks through earlier. Thereafter the adsorbed 3MP appears at the exit.

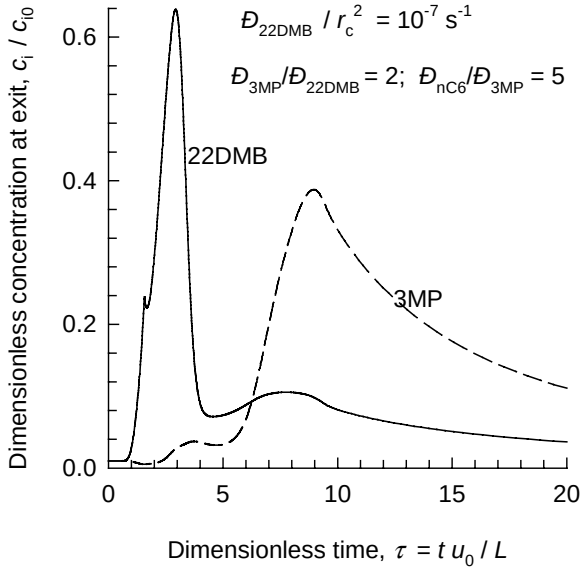

Fig. 15. Breakthrough in a pulsed chromatograph packed with MFI crystals. The temperature $T = 362$ K; the porosity of the packed bed $\varepsilon = 0.4$; length of packed bed $L = 0.4$ m; interstial gas velocity at inlet $u_0 = 0.0125$ m/s; density of MFI $\rho = 1800$ kg/m^3. The radius of the crystallites r_c was chosen such that $Đ_{C1}/r_c^2 = 10^{-7}$ s^{-1}. At time $t = 0$, the partial pressures of the adsorbing species, *n*C6, 3MP and 22DMB, at the inlet are maintained at 20 Pa, 20 kPa and 20 kPa, respectively. These conditions are maintained for 50 s. The initial loadings of the MFI crystals correspond to equilibrium at partial pressures of C1, C2, C3 and *n*C4 at 200 Pa. At $t = 50$ s, the partial pressures of C6, 3MP and 22DMB at the inlet are maintained at 60 kPa, 20 Pa and 20 Pa, respectively. The partial pressures of the non-adsorbing inerts are maintained such that the total pressure is 100 kPa.

Pulsed chromatography may therefore be used to separate di-branched from the mono-branched isomers of hexane.

5. Conclusions

In this paper we have developed a multi-scale modelling strategy for zeolitic process design. Molecular simulations (CBMC, KMC, MD) are used to generate the sorption and diffusion parameters, the Maxwell–Stefan diffusion equations bind these together and the solution of the transient equations of continuity yields the permeation fluxes and breakthrough curves required in process design. The multi-scale modelling strategy has been illustrated by means of several case studies involving transient permeation across zeolite membranes and breakthroughs in packed beds and pulsed chromatography columns.

The illustrative examples show that it is possible to exploit configurational entropy effects in developing novel processes for separating di-branched alkanes from mono-branched alkanes; such separations are of great importance in the petroleum industry.

The strategy outlined in the present paper will help to reduce process development times by reducing significantly the experimental effort required in process development.

Acknowledgements

The authors gratefully acknowledge grants from the Netherlands Organization for Scientific Research (NWO-CW).

References

Auerbach, S. M. (2000). Theory and simulation of jump dynamics, diffusion and phase equilibrium in nanopores. *International Reviews in Physical Chemistry*, *19*, 155–198.

Bakker, W. J. W. (1999). *Structured systems in gas separation*. Ph.D. thesis, Delft University of Technology, Delft.

Calero, S., Smit, B., & Krishna, R. (2001a). Configurational entropy effects during sorption of hexane isomers in silicalite. *Journal of Catalysis*, *202*, 395–401.

Calero, S., Smit, B., & Krishna, R. (2001b). Separation of linear, mono-methyl and di-methyl alkanes in the 5–7 carbon atom range by exploiting configurational entropy effects during sorption on silicalite-1. *Physical Chemistry Chemical Physics*, *3*, 4390–4398.

Demontis, P., & Suffritti, G. B. (1997). Structure and dynamics of zeolites investigated by molecular dynamics. *Chemical Reviews*, *97*, 2845–2878.

Denayer, J. F., Baron, G. V., Martens, J. A., & Jacobs, P. A. (1998). Chromatographic study of adsorption of *n*-alkanes on zeolites at high temperatures. *Journal of Physical Chemistry B*, *102*, 3077–3081.

Frenkel, D., & Smit, B. (2002). *Understanding molecular simulations: From algorithms to applications* (2nd ed.). San Diego: Academic Press.

Fuchs, A. H., & Cheetham, A. K. (2001). Adsorption of guest molecules in zeolitic materials: Computational aspects. *Journal of Physical Chemistry B*, *105*, 7375–7383.

Huddersman, K., & Klimczyk, M. (1996). Separation of branched hexane isomers using zeolite molecular sieves. *American Institute of Chemical Engineers Journal*, *42*, 405–408.

Kapteijn, F., Moulijn, J. A., & Krishna, R. (2000). The generalized Maxwell–Stefan model for diffusion in zeolites: Sorbate molecules with different saturation loadings. *Chemical Engineering Science*, *55*, 2923–2930.

Kärger, J., & Ruthven, D. M. (1992). *Diffusion in zeolites and other microporous solids*. New York: Wiley.

Keil, F. J., Krishna, R., & Coppens, M. O. (2000). Modeling of diffusion in zeolites. *Reviews in Chemical Engineering*, *16*, 71–197.

Krishna, R. (2001). Diffusion of binary mixtures across zeolite membranes: Entropy effects on permeation selectivity. *International Communications in Heat and Mass Transfer*, *28*, 337–346.

Krishna, R. (2002). Predicting transport diffusivities of binary mixtures in zeolites. *Chemical Physics Letters*, *355*, 483–489.

Krishna, R., & Paschek, D. (2002). Self-diffusivities in multicomponent mixtures in zeolites. *Physical Chemistry Chemical Physics*, *4*, 1891–1898.

Krishna, R., & Wesselingh, J. A. (1997). The Maxwell–Stefan approach to mass transfer. *Chemical Engineering Science*, *52*, 861–911.

Krishna, R., Calero, S., & Smit, B. (2002). Investigation of entropy effects during sorption of mixtures of alkanes in MFI zeolite. *Chemical Engineering Journal*, *88*, 81–94.

Maginn, E. J., Bell, A. T., & Theodorou, D. N. (1993). Transport diffusivity of methane in silicalite from equilibrium and nonequilibrium simulations. *Journal of Physical Chemistry*, *97*, 4173–4181.

Myers, A. L., & Prausnitz, J. M. (1965). Thermodynamics of mixed gas adsorption. *American Institute of Chemical Engineers Journal*, *11*, 121–130.

Ruthven, D. M., Farooq, S., & Knaebel, K. S. (1994). *Pressure swing adsorption*. New York: VCH Publishers.

Santilli, D. S. (1986). Pore probe: A new technique for measuring the concentration of molecules inside porous materials at elevated temperatures. *Journal of Catalysis*, *99*, 335–341.

Schenk, M., Vidal, S. L., Vlugt, T. J. H., Smit, B., & Krishna, R. (2001). Separation of alkane isomers by exploiting entropy effects during adsorption on silicalite-1: A configurational-bias Monte Carlo simulation study. *Langmuir*, *17*, 1558–1570.

Schuring, D., Koriabkina, A. O., de Jong, A. M., Smit, B., & van Santen, R. A. (2001). Adsorption and diffusion of *n*-hexane/2-methylpentane mixtures in zeolite silicalite: Experiments and modeling. *Journal of Physical Chemistry B*, *105*, 7690–7698.

Skoulidas, A. I., & Sholl, D. S. (2001). Direct tests of the Darken approximation for molecular diffusion in zeolites using equilibrium molecular dynamics. *Journal of Physical Chemistry B*, *105*, 3151–3154.

Snurr, R. Q., & Kärger, J. (1997). Molecular simulations and NMR measurements of binary diffusion in zeolites. *Journal of Physical Chemistry B*, *101*, 6469–6473.

Talu, O. (1998). Needs, status, techniques and problems with binary gas adsorption experiments. *Advances in Colloid and Interface Science*, *77*, 227–269.

van de Graaf, J. M., Kapteijn, F., & Moulijn, J. A. (1999). Modeling permeation of binary mixtures through zeolite membranes. *American Institute of Chemical Engineers Journal*, *45*, 497–511.

Vlugt, T. J. H., Krishna, R., & Smit, B. (1999). Molecular simulations of adsorption isotherms for linear and branched alkanes and their mixtures in silicalite. *Journal of Physical Chemistry B*, *103*, 1102–1118.

Vlugt, T. J. H., Martin, M. G., Smit, B., Siepmann, J. I., & Krishna, R. (1998). Improving the efficiency of the configurational-bias Monte Carlo algorithm. *Molecular Physics*, *94*, 727–733.

Webb, E. B., Grest, G. S., & Mondello, M. (1999). Intracrystalline diffusion of linear and branched alkanes in the zeolites TON, EUO, and MFI. *Journal of Physical Chemistry B*, *103*, 4949–4959.

Zhu, W., Kapteijn, F., & Moulijn, J. A. (2000). Adsorption of light alkanes on silicalite-1: Reconciliation of experimental data and molecular simulations. *Physical Chemistry Chemical Physics*, *2*, 1989–1995.